Technical Paper

Transactions of the Society of
Naval Architects of Korea
Vol. 31. No. 1, February 1994
大 韓 造 船 學 會 論 文 集
第 31 卷 第 1 號 1994年 2月

Stochastic Imperfection Sensitivity Analyses of Stiffened Cylindrical Shells with Geometric Random Imperfection

by

D.K. Kim* and Y.S. Yang**

불확정적인 초기형상결함을 갖는 보강 원통형 쉘의 확률론적 초기결함 민감도해석

김두기*, 양영순**

Abstract

In this paper, stochastic imperfection sensitivity analyses of stiffened cylindrical shells under static load are presented. Multimode formulation is performed for the buckling load calculation based on the Donnell' s theory and Galerkin approximation. Random imperfection field theory and response surface method are combined with deterministic buckling analysis scheme to perform stochastic imperfection sensitivity analyses of stiffened cylindrical shells considering random geometric imperfection. From the characteristics of probabilistic buckling load, the relation between reliability index and safety parameter can be obtained in addition to the relation between load and reliability index. Those results can be used to determine the range of required safety parameter and acceptable imperfection.

요 약

본 논문에서는 정하중을 받는 보강 원통형 쉘의 확률론적 초기결함 민감도 해석을 수행하였다. Donnell의 쉘이론, Galerkin 근사법에 의거 좌굴하중 도출을 위한 다중모드 정식화를 수행하고 이에 random한 기하학적 초기결함의 확률장 이론 및 응답면 기법을 결합하였다.

계산된 확률론적 좌굴하중 결과로부터 신뢰도 지수-하중, 신뢰도 지수-안전계수의 관계를 구할 수 있고 이를 이용하면 요구되는 안전계수의 범위, 허용가능 초기결함의 범위 설정이 가능 할 것이다.

Manuscript received : Aug. 23. 1993
Received manuscript received : Dec. 13. 1993

* Member, Agency for Defense Development
** Member, Seoul National University

1. Introduction

With the recent advances in offshore, aerospace and nuclear industry, rational structural design of shell structures based on more accurate strength prediction is required. Shell structures are good for the efficient increase of stiffness enabling lightweight structural design but are vulnerable to buckling failure. Cylindrical shells are used as the main structural components of offshore structures, airplanes and nuclear reactors. Initial postbuckling behavior of cylindrical shells is unstable under axial compressive loading and nonlinear coupling between buckling modes is dominant, so they become very sensitive to geometric initial imperfection. Much imperfection sensitivity studies from the deterministic viewpoint have been carried out to analyse the buckling strength reduction due to geometric imperfection. But in real shells, geometric imperfection shows random properties which cannot be described from the deterministic viewpoint. Therefore a stochastic approach is requisite to take into consideration of randomness of geometric imperfection rationally.

Since Bolotin[1], many researches have been performed to get more rational and practical strength prediction results by combining the imperfection sensitivity theory and probabilistic theory about geometric initial imperfection. First study about stochastic imperfection sensitivity of cylindrical shells was performed by Amazigo [2]. Since then Hansen[3], Fersht[4] treated general asymmetric random imperfection and others [5-7] performed buckling reliability studies of cylindrical shells.

Nowadays probabilistic finite element method appears powerful tool for structural reliability analysis[8], but stochastic imperfection sensitivity of shells has hardly been performed until now by the method. Many studies about stochastic imperfection sensitivity has been mainly confined on unstiffened cylindrical shell and applied on stiffened shell very recently. Recent researchers has doné stochastic imperfection sensitivity studies on stiffened shell by combining deterministic stability analysis methodology and reliability analysis technique, which was mainly Monte Carlo simulation method and Mean value first order second moment method(MVFOSM).

Monte Carlo simulation method is good for the exact reliability analysis but costs too much time for reliability calculation. MVFOSM is simple to apply but has weakness that failure probability changes according to the form of limit state equation.

In the reliability analysis of highly nonlinear problem, such as shell buckling with multimode geometric imperfection where the limit state equation is implicit and solution is sought iteratively per incremental loading, advanced first order second moment(AFOSM) is useful but diffucult to apply directly due to truncation error cumulation in the process of calculating the derivatives of random variables. In this paper to overcome these difficulies, response surface method, which is used in experiment design of statistics, is combined with the deterministic analysis algorithm based on Donnell's theory to perform stochastic imperfection sensitivity analyses of stiffened cylindrical shell under axial compressive load.

2. Deterministic Multimode for mulation

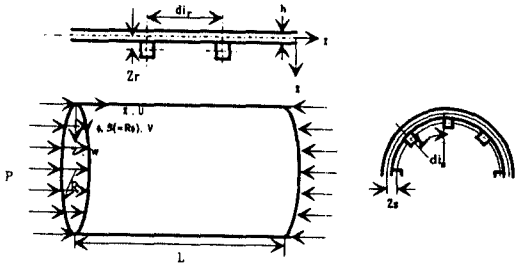

Fig. 1 Coordinate system and load

In Fig.1, geometric property, coordinate system, loading condition of stiffened cylindrical shell treated in this paper is presented. It is assumed that thin shell theory, shallow shell theo-

ry, Donnell' s theory can be applied and that the magnitude, change rate of geometric imperfection can be negligible compared with the radius of stiffened cylindrical shell. It is also assumed that the stiffener spacing is close enough for orthotropic shell theory to be applied and both edges are simply supported.

Nondimensional equlibrium and compatibility equation, boundary condition can be derived from virtual work theorem[9]. Nondimensional equilibrium equation and compatibility equation are

$$\hat{h}_{11}w_{,\xi\xi\xi\xi}+2\hat{h}_{12}w_{,\xi\xi\eta\eta}+\hat{h}_{22}w_{,\eta\eta\eta\eta}-\left[\hat{q}_{11}f_{,\xi\xi\xi\xi}+2\hat{q}_{12}f_{,\xi\xi\eta\eta}+\hat{q}_{22}f_{,\eta\eta\eta\eta}\right]-\alpha_1 cf_{,\xi\xi}-c\left[f_{,\xi\xi}(w+w_0)_{,\eta\eta}-2\beta_1{}^2 f_{,\xi\xi}(w+w_0)_{,\xi\eta}+\beta_1{}^4 f_{,\eta\eta}(w+w_0)_{,\xi\xi}\right]=0 \quad (1)$$

$$\hat{d}_{11}f_{,\xi\xi\xi\xi}+2\hat{d}_{12}f_{,\xi\xi\eta\eta}+\hat{d}_{22}f_{,\eta\eta\eta\eta}+\left[\hat{q}_{11}w_{,\xi\xi\xi\xi}+2\hat{q}_{12}w_{,\xi\xi\eta\eta}+\hat{q}_{22}w_{,\eta\eta\eta\eta}\right]+\frac{1}{2}c\beta_1{}^2\left[w_{,\xi\xi}(w+2w_0)_{,\eta\eta}-2w_{,\xi\eta}(w+2w_0)_{,\xi\eta}+w_{,\eta\eta}(w+2w_0)_{,\xi\xi}\right]+c\alpha_1 w_{,\xi\xi}=0 \quad (2)$$

where nondimensional coefficients are

$$\xi=\frac{\pi x}{L},\ \eta=\frac{\pi s}{l},\quad l=\pi R,\quad w=\frac{w}{h},\quad w_0=\frac{w_0}{h}$$

$$f=\frac{F}{Eh^3},\ \alpha_1=\frac{L^2}{\pi^2 Rh},\ \beta_1=\frac{L}{\pi R},\ c=12(1-\nu^2)$$

$$Z=\frac{\sqrt{1-\nu^2}L^2}{Rh},\quad P_{cl}=\frac{2\pi Eh^2}{\sqrt{3(1-\nu^2)}},\quad \Xi=\frac{P}{P_{cl}}$$

$$\sigma=\frac{PL^2}{\pi^3 ERh^3},\quad \hat{e}_u=\frac{he_u}{2\pi R},\quad (u,v)=\frac{L}{\pi h^2}(U,V)$$

$$\hat{h}_{11}=h_{11},\quad \hat{h}_{12}=h_{12}\beta_1{}^2,\quad \hat{h}_{22}=h_{22}\beta_1{}^4$$

$$\hat{q}_{11}=\frac{c}{h}q_{11},\quad \hat{q}_{12}=\frac{c}{h}\beta_1{}^2 q_{12},\quad \hat{q}_{22}=\frac{c}{h}\beta_1{}^4 q_{22}$$

$$\hat{d}_{11}=Ehcd_{11},\quad \hat{d}_{12}=Ehcd_{12},\quad \hat{d}_{22}=Ehcd_{22}$$

$$h_{22}=1+L_r-\frac{12}{h^2}\frac{z_r^2K_r^2}{\alpha}(1+K_s)$$

$$q_{11}=-\frac{\nu z_s K_s}{\alpha}$$

$$q_{12}=\frac{\left[(1+K_r)z_sK_s+(1+K_s)z_rK_r\right]}{2\alpha}$$

$$q_{22}=-\frac{\nu z_r K_r}{\alpha},\quad d_{11}=\frac{(1+k_s)}{\alpha D_1}$$

$$d_{12}=\frac{\left[(1+K_s)(1+K_r)-\nu\right]}{\alpha(1-\nu)D_1},\quad d_{22}=\frac{(1+k_r)}{\alpha D_1}$$

$$D_1=\frac{Eh}{1-\nu^2},\quad D=\frac{Eh^3}{12(1-\nu^2)}$$

$$\alpha=\left[(1+K_r)(1+K_s)-\nu^2\right]$$

$$K_s=\frac{A_s(1-\nu^2)}{hdi_s},\quad K_r=\frac{A_r(1-\nu^2)}{hdi_r}$$

$$L_s=\frac{EI_{os}}{Ddi_s},\quad L_r=\frac{EI_{or}}{Ddi_r}$$

Boundary conditions are

$$w=0\quad at\quad \xi=0,\ \pi \quad (3)$$

$$(1+L_s)w_{,\xi\xi}+\beta_1{}^2\nu w_{,\eta\eta}-12\hat{z}_s k_s\left[\hat{a}_1 f_{,\eta\eta}+\hat{a}_2 f_{,\xi\xi}+\hat{a}_3 w_{,\xi\xi}+\hat{a}_4 w_{,\eta\eta}\right]=0\quad at\quad \xi=o,\pi \quad (4)$$

$$\hat{b}_1 f_{,\eta\eta}+\hat{b}_2 f_{,\xi\xi}+\hat{b}_3 w_{,\xi\xi}+\hat{b}_4 w_{,\eta\eta}+\alpha_1 w-\frac{1}{2}\beta_1{}^2 w,\eta^2-\beta_1{}^2 w_{,\eta}\,w_{0,\eta}=0\quad at\quad \xi=0,\pi \quad (5)$$

where $\hat{a}_1 \ldots \hat{b}_4$ are

$$\hat{a}_1=a_1 Eh\beta_1{}^2,\ \hat{a}_2=a_2 Eh,\ \hat{a}_3=\frac{a_3}{h},\ \hat{a}_4=\frac{\beta_1{}^2}{h}a_4$$

$$\hat{b}_1=b_1 Eh\beta_1{}^2,\ \hat{b}_2=b_2 Eh,\ \hat{b}_3=\frac{b_3}{h},\ \hat{b}_4=\frac{\beta_1{}^2}{h}b_4$$

$$a_1=\frac{(1+K_r)}{\alpha D_1},\quad a_2=-\frac{\nu}{\alpha D_1},$$

$$a_3=\frac{(1+K_r)z_sK_s}{\alpha},\quad a_4=-\frac{\nu z_r K_r}{\alpha}$$

$$b_1=-\frac{\nu}{\alpha D_1},\quad b_2=\frac{(1+K_s)}{\alpha D_1},\quad b_3=-\frac{\nu z_s K_s}{\alpha}$$

$$b_4 = (1+K_s)z_r K_r$$

Load condition equation is

$$\int_0^{2\pi} f_{,\eta\eta} \; d\eta = -\sigma \quad at \quad \xi = 0, \pi \tag{6}$$

Circularity condition is

$$\int_0^{2\pi} \frac{\partial v}{\partial \eta} d\eta = 0 \tag{7}$$

w, w_0 satisfying simple support condition can be written like Eq. (8).

$$\begin{aligned} w &= \sum_{m=1}^{NM} a_{n1(m),n2(m)} \sin n1(m)\xi \cos n2(m)\eta \\ w_0 &= \sum_{m=1}^{NM} c_{n1(m),n2(m)} \sin n1(m)\xi \cos n2(m)\eta \end{aligned} \tag{8}$$

where NM means the number of buckling modes considered, n1(m) m-th longitudinal half wave number, n2(m) m-th cirdumferential full wave number respectively. By substituting Eq. (8) into Eq. (2)-(7), nondimensionalized stress function f can be obtained. After substituting f into the equilibrium equation and performing Galerkin integration with respect to each buckling mode, nonlinear coupled algebraic equation can be obtained. Since the equation is nonlinear equation of multimode generalized ccordinates under given load condition, the exact solution can hardly be obtained and so an approximate solution can be obtained by iteration under given load condition.

In case $a^{(i,r+1)}_{n1(m),n2(m)}$ (m=1, , , NM) means (r+1)-th approximate solution under i-th load Ξ^i, it can be written as follows according to Newton's quasi-linearization theorem.

$$a^{(i,r+1)}_{n1(m),n2(m)} = a^{(i,r)}_{n1(m),n2(m)} + \delta a^{(i,r)}_{n1(m),n2(m)}, (\mathrm{m}=1, , , \mathrm{NM}) \tag{9}$$

After substituting Eq. (9) to Eq. (1) and neglecting higher-order terms, Eq. (1) can be written as the following matrix equation.

$$[K]^{(i)} \quad \{\delta a\}^{(i,r)} = -\{R\}^{(i,r)} \tag{10}$$

where [K] means stiffness matrix which is nonlinear function of Ξ, $a_{n1(m),n2(m)}$, $c_{n1(m),n2(m)}$ (m=1, , , NM), $\{\delta a\}$ incremental generalized ccordinate matrix and {R} residual force matrix. The solution in i-th load can be obtained if the norm of {R} satisfy the convergence criteria and the solution is used as the first guess for solution of (i+1)-th load step. By repeating the above process, buckling load can be obtained.

3. Probabilistic Charateristics of Geometric Imperfection

As geometric initial imperfection can be written as Eq. (8), the mean of the inperfection can be written as follows.

$$\begin{aligned} &E[w_0(\xi,\eta)] \\ &= \sum_{m=1}^{NM} E\left[c_{n1(m),n2(m)}\right] \sin n1(m)\xi \cos n2(m)\eta \end{aligned} \tag{11}$$

$$E\left[c_{n1(m),n2(m)}\right]^{(e)} = \frac{1}{M}\sum_{m=1}^{M} c_{n1(m),n2(m)} \tag{12}$$

where superscript(e) means ensemble, M the size of discrete data.

Covariance function can be written as follows.

$$\begin{aligned} &R_{w_0}(\xi_1,\eta_1;\xi_2,\eta_2) \\ &= E\left[\left[w_0(\xi_1,\eta_1) - E\left[w_0(\xi_1,\eta_1)\right]\right]\left[w_0(\xi_2,\eta_2) - E\left[w_0(\xi_2,\eta_2)\right]\right]\right] \\ &= E\left[\left(\sum_{m=1}^{NM}\left(c_{n1(m),n2(m)} - E\left[c_{n1(m),n2(m)}\right]\right)\sin n1(m)\xi \cos n2(m)\eta\right)\right. \\ &\quad \left.\left(\sum_{p=1}^{NM}\left(c_{n1(p),n2(p)} - E\left[c_{n1(p),n2(p)}\right]\right)\sin n1(p)\xi \cos n2(p)\eta\right)\right] \\ &= \sum_{m=1}^{NM}\sum_{P=1}^{NM} S_{m,p} \sin n1(m)\xi \cos n2(m)\eta \sin n1(p)\xi \cos n2(p)\eta \end{aligned} \tag{13}$$

where $S_{m,p}$ means the element of variance-covariance matrix[S].

$$S^{(e)}_{m,p} = \frac{1}{M-1}\sum_{m=1}^{M}\sum_{P=1}^{M}\left[\left(c_{n1(m),n2(m)} - E\left[c_{n1(m),n2(m)}\right]^{(e)}\right)\left(c_{n1(p),n2(p)} - E\left[c_{n1(p),n2(p)}\right]^{(e)}\right)\right] \tag{14}$$

4. Reliability Analysis Method

4.1 Definition of failure probability

When $\bar{x}$ means basic random variable vector affecting structural safety and $f_{\bar{x}}(x_1, \ , \ , x_n)$ joint probability density function of the variables, structural failure probability P_f can be written as follows

$$P_f = 1 - \int_D f_{\bar{x}}(x_1, \ , \ , x_n)\ dD \tag{15}$$

where D means safe zone of structure.
Hyperplane dividing the safe and unsafe zone in the n-dimensional space of basic random variables means failure surface and the equation expressing the failure surface means the limit state equation. Limit state equation Z can be written as follows.

$$Z = G(\bar{x}) = 0 \tag{16}$$

where $G(\bar{x})$ means state function. After obtaining probability density function or distribution function by using joint probability density function of $\bar{x}$, the probability can be calculated in case of $Z < 0$, which means failure probability

4.2 Approximate reliability analysis method

The calculation of failure probability using Eq. (15) is most accurate, but joint probability density function of basic random variables cannot be generally known and mutiple integration, if known, entails much difficulty. Therefore to evade the difficulty, approximate method have to be used, the typical of which are MVFOSM and AFOSM. MVFOSM has several problems that failure probability can be changed with the change of limit state equation and cannot be calculated in case of nonnormal random variables.

Hasofer & Lind[10] overcame these problems by proposing AFOSM, in which basic random variables are transformed into new normalized variables of Gaussian distribution and failure surface is linearly approximated at the most probable failure point which lies nearest from the origin. Though the failure probability obtained by AFOSM is more accurate than that by MVFOSM, direct application to complex nonlinear structure entails much difficulty.

4.3 Simulation method

Monte Carlo simulation method(MCM) is widely used with the approximate method. In the method probability density function of the state function is obtatined using the original form of state function. The value of random variables are generated according to the respective probability density function and these variables are used for the calculation of the state function, statistical analysis of which gives probability density function of state function. As only the value of state function is necessary in this method, it can be used for the reliability analysis of the complex structure. But the method has the weakness that it costs too much time for reliability calculation.

4.4 Response surface method(RSM)

It is basic concept of RSM to convert real complicated limit state equation $Z(\bar{x})$ into proper polynomial $\bar{Z}(\bar{x})$. When Z is expressed as a function of $\bar{x}(x_1, \ , \ , x_n)$ its Taylor expansion around mean value point $\bar{x}_0$ becomes

$$Z(\bar{x}) = Z(\bar{x}_0) + \sum_{i=1}^{n}\left(\frac{\partial Z}{\partial x_i}\right)x_i + \frac{1}{2}\sum_{i=1}^{n}\sum_{j=1}^{n}\left(\frac{\partial^2 Z}{\partial x_i\,\partial x_j}\right)x_i x_j + \sum_{i=1}^{n}\Delta_i \tag{17}$$

Eq. (17) becomes polynomial regression model. According to Bucher's proposal[11], the coupled terms can be neglected.

$$Z(\bar{x}) = c_0 + \sum_{i=1}^{n} c_i x_i + \sum_{i=1}^{n} c_{ii} x_i^2 + \sum_{i=1}^{n}\Delta_i \tag{18}$$

where

$$Z(\bar{x}_0) = c_0$$

$$\frac{\partial Z}{\partial x_i} \Big|_{\bar{x}=\bar{x}_0} = c_i$$

$$\frac{1}{2}\frac{\partial^2 Z}{\partial x_i \partial x_j} \Big|_{\bar{x}=\bar{x}_0} = c_{ij}$$

In Eq. (18) x_i is sampling point at which limit state equation is evaluated in the interest domain. They are generally $E[x_i]$ and $E[x_i] \pm k\sigma$, where $E[x_i]$ means mean value of x_i, σ_i standard deviation of x_i, k arbitrary real number.

The number of sampling points necessary to get Eq. (18) is (2n+1). RSM is more efficient than approximate method or simulation method where faiulure probability can be calculated if limit state equation is evaluated as many times as the number of sampling points.

Eq. (18) can be expressed as the following matrix form.

$$[Z] = [x][c] + [\Delta] \tag{19}$$

where

$$[Z] = [Z^1 \ Z^2 \ \cdots \ Z^N]^T$$

$$[x] = [[Y_1][Y_2] \ \cdots \ [Y_N]]^T$$

$$[Y_i] = [1 \ x_i^1 \ \cdots \ x_i^N (x_i^1)^2 \ \cdots \ (x_i^N)^2]$$

$$[c] = [c_0 \ c_1 \ \cdots \ c_{11} \ \cdots \ c_{NN}]^T$$

$$[\Delta] = [\Delta^1 \ \Delta^2 \ \cdots \ \Delta^N]^T$$

and N means (2n+1), superscripts the values of random variables and limit state equation at the sampling points. If the error square is differentiated with respect to $[c]$, $[c]_{final}$ which satisfies minimization condition can be expressed as follows.

$$[c]_{final} = ([x][x]^T)^{-1}[x]^T[Z] \tag{20}$$

Therefore the approximated limit state equation becomes

$$\bar{Z} = [x'][c]_{final} \tag{21}$$

$$[x'] = [1 \ x_1 \ \cdots \ x_n (x_1)^2 \ \cdots \ (x_n)^2]$$

With Eq. (21) and AFOSM, first order approximate failure point on the failure surface $[\bar{x}_D]$ can be obtained. With additional extrapolation around $[\bar{x}_D]$, new starting point $[x^M]$ is obtained. Similar process is repeated until final failure probability can be obtained.

5. Numerical Calculation and Discussion

As the first example, relation between nondimensional load and buckling failure probability is analized considering only the geometric imperfection as the random variable. In Table 1 mean value and coefficient of variation (COV) of geometric imperfection are listed for each analysis case. In Table 2 geometric and material characteristics of the shell are listed. The relation between nondimensional load and buckling failure probability are shown in Fig.2 and Fig.3. The larger COV of geometric imperfection gives greater buckling probability when external load is below deterministic buckling load. When load is above the deterministic buckling load, the reverse is true.

Phenomena above mentioned means that in the postbuckling range the case with greater COV can search new stability point more easily than the case with less COV. Histogram of probabilistic buckling load for the typical case is presented in Fig.4, the distribution of which is similar to normal distribution. In Fig.5, stochastic imperfection sensitivity analysis result by RSM is compared with that by MCM for the case 2 of Table 1. Both results are very similar, which shows that RSM in this paper gives very exact reliability analysis results. Also RSM reduces computer time very much comparing with MCM as can be shown in Table 3.

As the element affecting buckling probability of stiffened cylindrical shell, many parameters such as elasticity modulus, stiffener section

area, moment of inertia of stiffener except geometric imperfection can be considered. Reliability analysis result considering elasticity modulus as additional random variable is compared with results considering only geometric imperfection in Fig.6. Both results are nearly same, which shows that elasticity modulus has negligible effect on buckling probability of stiffened shell under axial compresion. Stringer section area has random property and analysis result considering stringer section area as additional random variable is compared with results considering only geometric imperfection in Fig.7, Fig.8. As can be shown, the effect of stringer section area on the buckling probability is definite in case of small COV of geometric imperfection and its effect is rather diminished with the increase of COV of geometric imperfection.

The above results coincides with the result by Lin[13] for the 2-dimensional frame structures with geometric imperfection. As can be shown in Fig.9, moment of inertia of stringer section area has a negligible effect on the buckling probability. In Fig.10, histogram of buckling load is shown for the case considering moment of inertia of stringer section as an additional random variable.

Buckling probability can be considered to have a normal distribution charateristics, which can be confirmed from the various results. Therefore the relation between reliability index and buckling probability can be utilized to get a useful result. The relation between reliability index and failure probability P_f can be presented as follows.

$$\beta = -\Phi^{-1}(P_f) \tag{22}$$

where

Φ ; *Normal cumulative distribution function*

P_f ; *Failure probability*

In Fig.11 the relation between external load and reliability index is shown for 3 cases in Table 1. It is recognized that reliability index decreases with the increase of COV. In Fig.12 the relation between safety parameter and is shown, from which it is recognized that larger safety parameter is required to have the same reliability index with the increase of COV of geometric imperfection.

With the increase of the number of geometric imperfection modes, analysis for the characteristics of failure probability was performed as Table 4. In Fig.13 the relation between load and failure probability with the change of COV of each mode is shown, the trend of which is nearly the same as that of case 1 & 2.

In Fig.14 the relation between reliability index and load is shown with the increase of number of imperfection modes for 2 cases in Table 4 are shown. Greater safety parameters are required to have the same reliability index with the increase of COV.

In Fig.15 the failure probability trend for the case with modal correlation is compared with that for the case without correlation, which shows little difference. Therefore it can be recognized that the effect of correlation between imperfection modes is negligible. In Fig. 16 failure probability trend are shown with the increase of modes number. Generally the results with the increased number of imperfection modes is shown to translate parallel to the load axis. The analysis for the real shell with multimode imperfections is performed using data of Arbocz[7] in Table 5. The imperfection modes and corresponding Fourier coefficients are contained in Table 6. In Fig.17 the reliability analysis result for the Arbocz shells by RSM in this paper is compared with that by MCM and it is recognized that two results are nearly the same.

Simple calculations are performed for the typical case of ring-stiffened shell. In Table 7 the geometric and material characteristics are contained for the ring-stiffened shell B1. Buckling probability is calculated and presented in Fig.18 for the case in which only geometric im-

perfection is random variable and differs in COV.

The general trend is shown to be similar to that for the stringer-stiffened shell. The characteristics of random variables are presented in Table 8. Reliability analysis is performed considering ring section area as additional random variable and characteristics of random variables, reliability results are shown in Table 8, Fig.19-20 respectively.

It is recognized that the effect of COV of geometric imperfection is definite for the low COV but it decreases with the increase of COV.

In Fig.21 the relation between load and reliability index for the case 2 in Table 8 is shown and it is recognized that reliability index is reduced with increase of COV of geometric imperfection under the same load. In Fig.22 the relation between safety parameter and for the same case is shown and it is shown that larger safety parameter is required to get the same reliability index with the increase of COV of geometric imperfection.

Table 1 Reliability analysis cases for shell S1

Random Var. / Case	$C_{(10,0)}$	$C_{(1,10)}$	E (Kgf/mm^2)	$A_s(mm^2)$	$I_s(mm^2)$
1	mean 0.03 c.o.v. 0.1	mean 0.3 c.o.v. 0.1	mean 6.89E3 c.o.v. 0.0	mean 0.795 c.o.v. 0.0	mean 0.149E-1 c.o.v. 0.0
2	mean 0.03 c.o.v. 0.3	mean 0.3 c.o.v. 0.3	mean 6.89E3 c.o.v. 0.0	mean 0.795 c.o.v. 0.0	mean 0.149E-1 c.o.v. 0.0
3	mean 0.03 c.o.v. 0.6	mean 0.3 c.o.v. 0.6	mean 6.89E3 c.o.v. 0.0	mean 0.795 c.o.v. 0.0	mean 0.149E-1 c.o.v. 0.0
4	mean 0.05 c.o.v. 0.1	mean 0.5 c.o.v. 0.1	mean 6.89E3 c.o.v. 0.0	mean 0.795 c.o.v. 0.0	mean 0.149E-1 c.o.v. 0.0
5	mean 0.05 c.o.v. 0.3	mean 0.5 c.o.v. 0.3	mean 6.89E3 c.o.v. 0.0	mean 0.795 c.o.v. 0.0	mean 0.149E-1 c.o.v. 0.0
6	mean 0.05 c.o.v. 0.6	mean 0.5 c.o.v. 0.6	mean 6.89E3 c.o.v. 0.0	mean 0.795 c.o.v. 0.0	mean 0.149E-1 c.o.v. 0.0
ES2	mean 0.03 c.o.v. 0.3	mean 0.3 c.o.v. 0.3	mean 6.89E3 c.o.v. 0.0	mean 0.795 c.o.v. 0.0	mean 0.149E-1 c.o.v. 0.0
AS1	mean 0.03 c.o.v. 0.1	mean 0.3 c.o.v. 0.1	mean 6.89E3 c.o.v. 0.0	mean 0.795 c.o.v. 0.1	mean 0.149E-1 c.o.v. 0.0
AS2	mean 0.03 c.o.v. 0.3	mean 0.3 c.o.v. 0.1	mean 6.89E3 c.o.v. 0.0	mean 0.795 c.o.v. 0.3	mean 0.149E-1 c.o.v. 0.0
IS2	mean 0.03 c.o.v. 0.3	mean 0.3 c.o.v. 0.3	mean 6.89E3 c.o.v. 0.0	mean 0.795 c.o.v. 0.0	mean 0.149E-1 c.o.v. 0.0

Table 2 Geometric & material charateristics of stringer stiffened shell S1

Item	Value
L(mm)	140.26
L/R	1.38
R/h	518.37
di_s/R	0.0625
Z_s/h	-1.709
A_s/di_gh	0.638
I_{so}/di_gh^3	0.311
Elastic Modulus E(Kgf/mm^2)	6.89E3
Poisson's Ratio	0.3
Batdorf Parameter	942.1

Table 3 Comparison of calculation time for case 2 (Alliant FX - 2812)

Monte Carlo Method (10,000 times)	266 sec.
Response surface method	16 sec.

Table 4 Reliability analysis case with multi mode imperfections as random variables for shell S1

Case	$c_{(10,0)}$	$c_{(1,10)}$	$c_{(1,9)}$	$c_{(1,8)}$	Correlation Coefficient
TR1	mean 0.03 c.o.v. 0.1	mean 0.3 c.o.v. 0.1	mean 0.3 c.o.v. 0.1	mean 0.3 c.o.v. 0.1	0.0
TR2	mean 0.03 c.o.v. 0.3	mean 0.3 c.o.v. 0.3	mean 0.3 c.o.v. 0.3	mean 0.3 c.o.v. 0.3	0.0
TR3	mean 0.03 c.o.v. 0.1	mean 0.3 c.o.v. 0.3	mean 0.3 c.o.v. 0.3	mean 0.3 c.o.v. 0.3	0.1

Table 5 Geometric and material properties of Arbocz shell

shell	h(mm)	A_s(mm^2)	Z_s(mm)	I_{so}(mm^4×100)	J_s(mm^4×100)	dis_s(mm)
SA2	0.1966	0.7987	0.3368	1.5038	4.9448	8.0239
SA3	0.2807	0.7472	0.3614	1.2033	4.0146	8.0289
SA4	0.2593	0.4890	0.2758	0.3474	1.1283	8.0112

Table 6 Values of the equivalent Fourier coefficient

Four. Coeff. \ Shell	SA2	SA3	SA4
C(1,2)	0.33691	0.08298	0.54217
C(1,9)	0.08843	0.02445	0.00297
C(1,10)	0.05524	0.03148	0.00414
C(1,11)	0.05494	0.01912	0.00502
C(1,19)	0.01106	0.00689	0.00424
C(1,21)	0.00879	0.00475	0.00095

Table 7 Geometric & material charateristics of ring stiffened shell B1

Item	Value
L(mm)	130.10
L/R	1.31
R/h	430.51
dis_s/R	0.309
Z_s/h	-1.127
A_r/dish	0.0414
I_{ro}/dish^3	0.311
Elastic Modulus (Kgf/mm^2)	6.89E3
Poisson's Ratio	0.3
Batdorf Parameter	942.1

Table 8 Reliability analysis cases for shell B1

Case \ Random variable	C(16,0)	C(1,8)	Ar(mm^2)
R1	mean 0.01 c.o.v. 0.1	mean 0.1 c.o.v. 0.1	mean 0.01 c.o.v. 0.0
R2	mean 0.01 c.o.v. 0.3	mean 0.1 c.o.v. 0.3	mean 0.307 c.o.v. 0.0
AR1	mean 0.01 c.o.v. 0.1	mean 0.1 c.o.v. 0.1	mean 0.307 c.o.v. 0.1
AR2	mean 0.01 c.o.v. 0.3	mean 0.1 c.o.v. 0.3	mean 0.307 c.o.v. 0.3

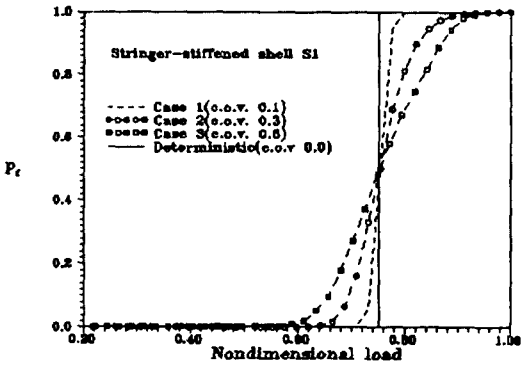

Fig. 2 Load v.s. buckling probability relation of shell S1 (case 1,2,3)

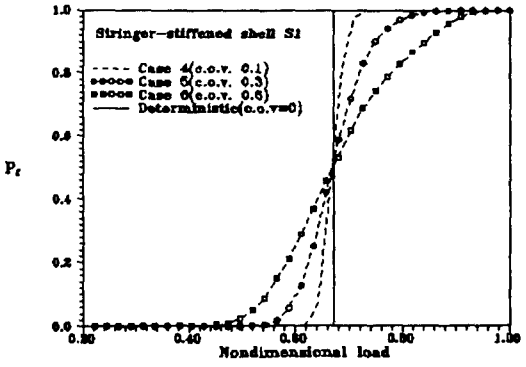

Fig. 3 Load v.s. buckling probability relation of shell (case 4, 5, 6)

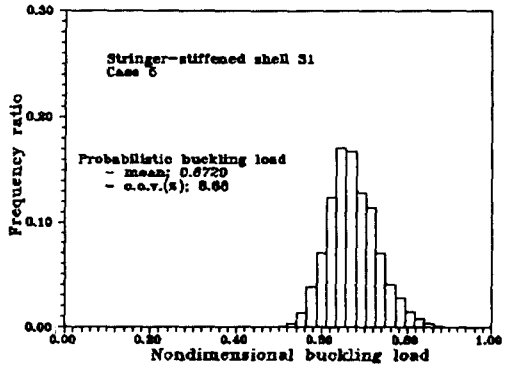

Fig. 4 Histogram of buckling load S1 for case 5

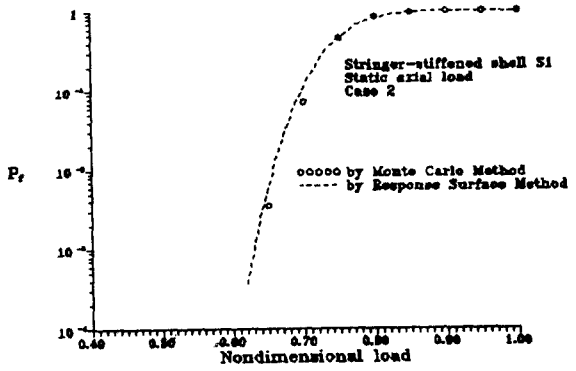

Fig. 5 Result comparison with that by Monte Carlo Method (shell S1, case 2)

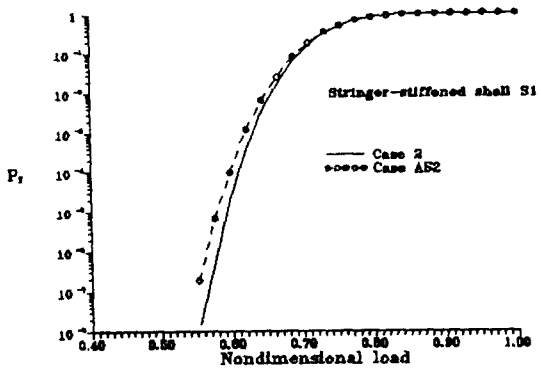

Fig. 8 Effect of stringer section area on the buckling probability of shell S1(comparison of case 2 & AS2)

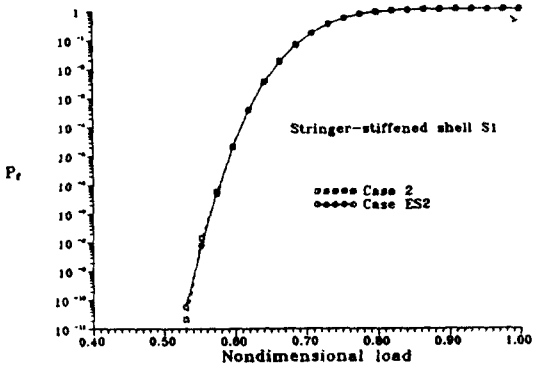

Fig. 6 Effect of elastic modulus on the buckling probability of shell S1(comparison of case 2 & ES2)

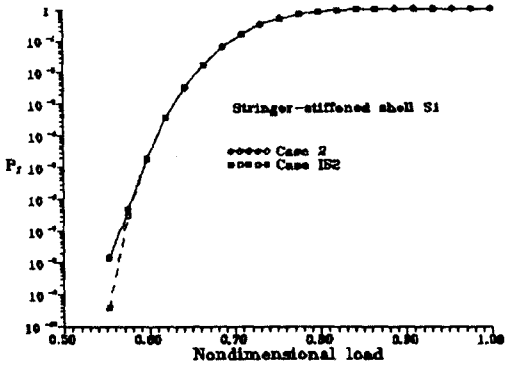

Fig. 9 Effect of L_s on the buckling probability of shell S1(comparison of case 2 & IS2)

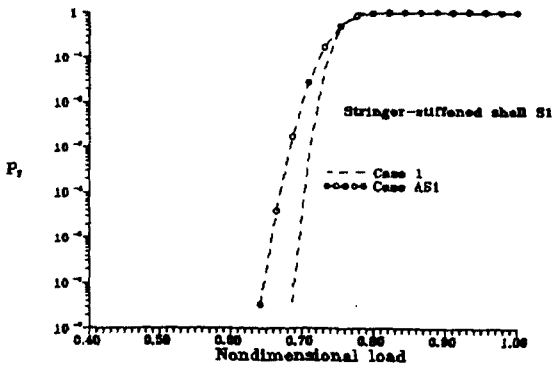

Fig. 7 Effect of stringer section area on the buckling probability of S1 (case 1 & AS1)

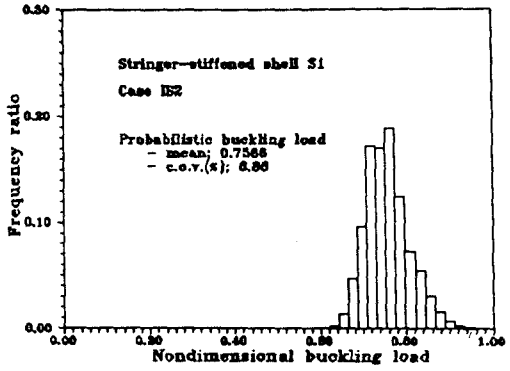

Fig. 10 Histogram of the buckling load of shell S1 (case IS2)

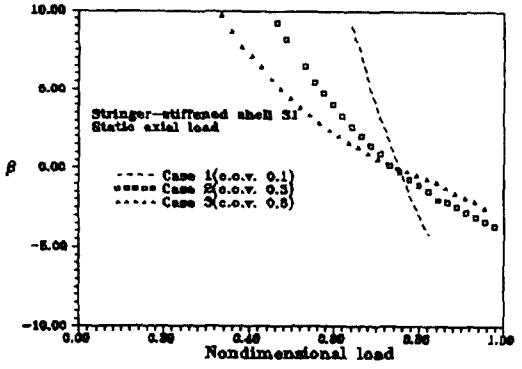

Fig. 11 Load v.s. reliability index β relation of shell S1 for case 1, 2, 3

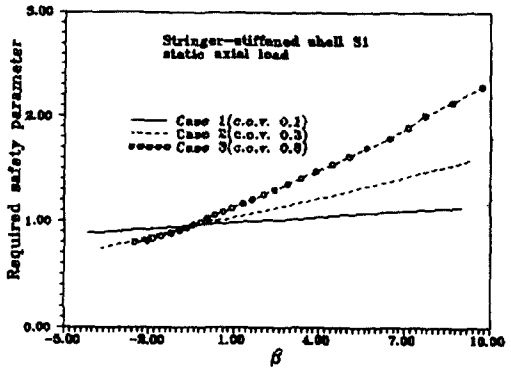

Fig. 12 β v.s. safety parameter relation of shell S1 for case 1, 2, 3

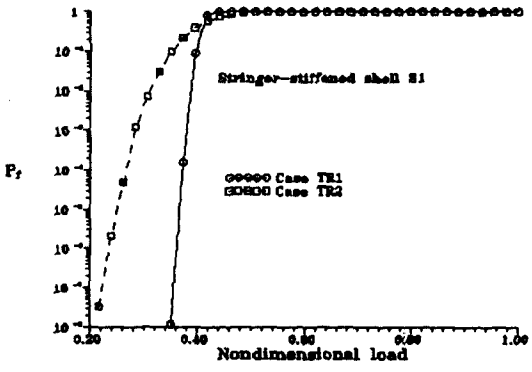

Fig. 13 Load v.s. P_f relation of shell s1 (case TRI, TR2)

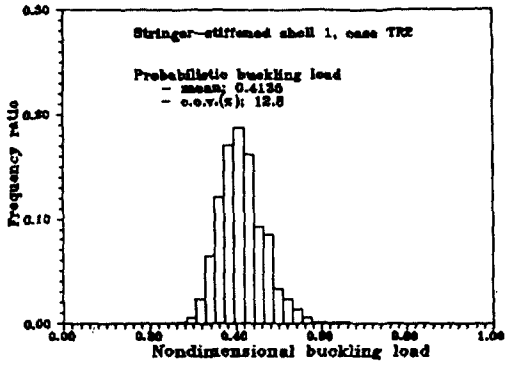

Fig. 14 Histogram of buckling load of shell S1 (case TR2)

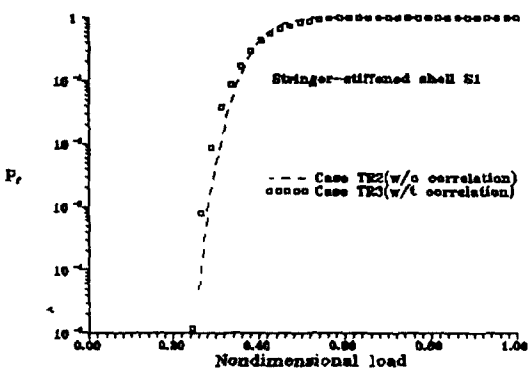

Fig. 15 Effect of correlation btwn random imperfection modes of shell S1

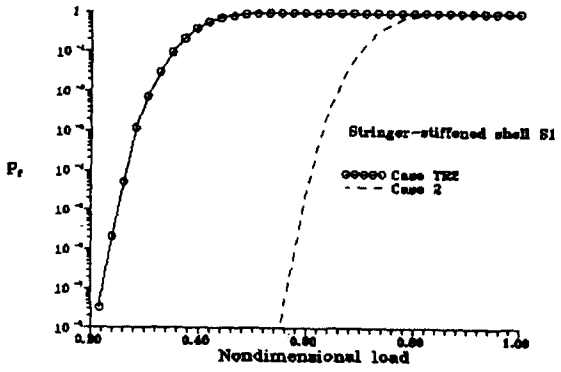

Fig. 16 Effect of imperfection mode increase for shell S1 (comparison of case 2 & TR2)

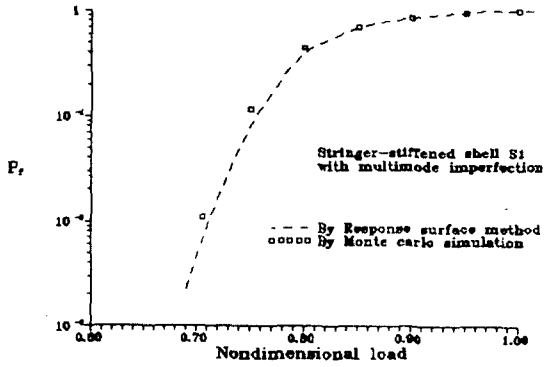

Fig. 17 Reliability analysis results for Arbocz shells

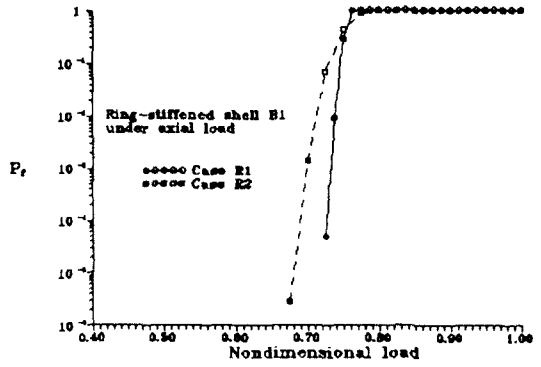

Fig. 18 Load v.s. buckling probability relation of shell B1 (case R1 & R2)

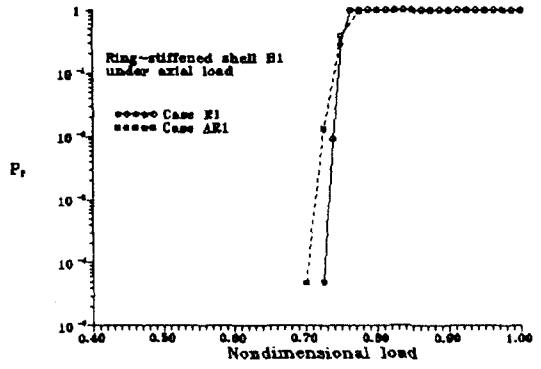

Fig. 19 Load v.s. buckling probability relation of shell B1 (comparison of case R1 & AR1)

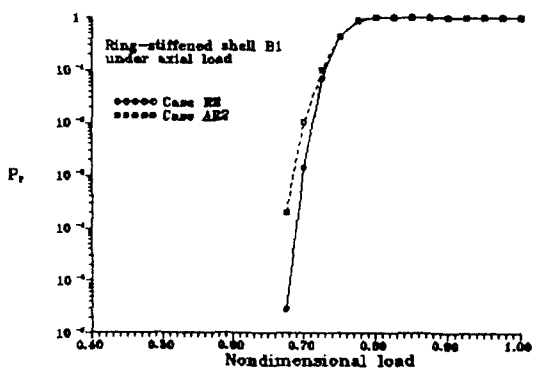

Fig. 20 Load v.s. buckling probability relation of shell B1(comparison of case R2 & AR2)

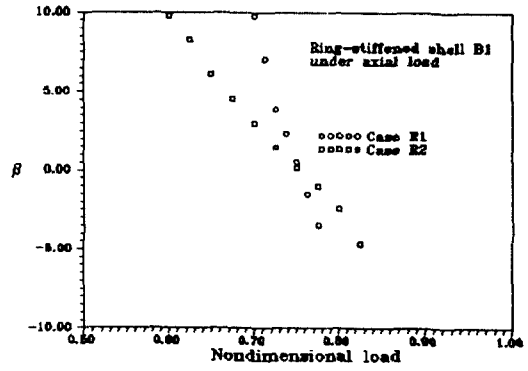

Fig. 21 Load v.s. β relation of shell B1 (case R1 & R2)

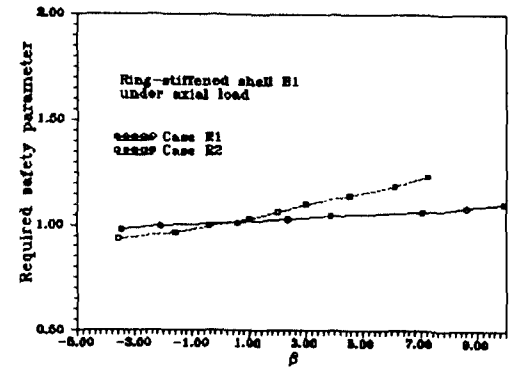

Fig. 22 β v.s. safety parameter relation of shell B1 (case R1 & R2)

6. Concluding Remarks

In this paper RSM, which can overcome the problems of conventional reliability analysis method is combined, with the multimode analysis algorithm to perform the stochastic imperfection sensitivity analysis of stiffened cylindrical shells and its validity and efficiency are confirmed. Buckling failure probability increases with the increase of mean value, COV, mode number of geometric imperfection under the same external load. Required safety parameter increases to get equal reliability index. Effect of random variables other than geometric imperfection on the buckling probability is analysed and stiffener section area is recognized as an important random variable for the determination of buckling probability. Distribution of buckling load of various cases is recognized similar to normal distribution. From the characteristics of probabilistic buckling load, relation between reliability index and safety parameter can be obtained in addition to the relation between load and reliability index. Those results can be used to determine the range of required safety parameter and acceptable imperfection.

References

[1] Bolotin V. V., "Statistical methods in structural mechanics", Holden-Day, 1969.

[2] Amazigo J. C., "Buckling under axial compression of long cylindrical shells with random axisymmetric imperfections", *Q. of Applied Mathematics*, Vol. 26, 537-566, 1969.

[3] Fersht R. S., "Buckling of cylindrical shells with random imperfections in 'Thin Shell Structure'", 325-341, Prentice-Hall, 1974.

[4] Hansen J. S., "General random imperfections in the buckling of axially loaded cylindrical shells", *AIAA Journal*, Vol. 15, No. 9, 250-266, 1977.

[5] Elishakoff I., "First-order second moment analysis of the buckling of shells with random imperfections", *AIAA Journal*, Vol. 25, No. 8, 1250-1256, 1987.

[6] Cryssantopoulos M. K. et al., "Imperfection modeling for buckling analysis of stiffened cylinders", *Journal of Structural Engineering, ASCE*, Vol. 117, No. 7, July, 1998-2027, 1991.

[7] Arbocz J., "Collapse of axially compressed cylindrical shells with random imperfec-tions", *AIAA Journal*, Vol. 29, No. 12, 2247-2256, 1991.

[8] Liaw D. G. et al, "Reliability of randomly imperfect beam-columns", *J. of Engineering Mechanics*, Vol. 15, No. 10, 2251-2270, 1989.

[9] Kim D. K., "Stochastic imperfection sensitivity analyses of stiffened cylindrical shells" Ph. D. Dissertation, Seoul National Univ., 1993.

[10] Hasofer A. M. and Lind N. C., "Exact and invariant second moment code format," *J. of Engineering Mechanics Division*, ASCE, Vol. 100, No. EM1, 111-121, 1974.

[11] Parkinson D. B., "Solution for second moment reliability index", *J. of the Engineering Mechanics Division, ASCE*, Vol. 104, No. EM 5, 1267-1275, 1978.

[12] Bucher C. G. and Bourgund U., "A fast and efficient response surface approach for structural reliability problems", *Structural Safety*, Vol. 7, 57-66, 1990.

[13] Lin S. C. and Kam T. Y., "Buckling failure probablity of imperfect elastic frames", *Computers and structures*, Vol. 44, No. 3, 515-524, 1992.